JOURNAL OF GUIDANCE, CONTROL, AND DYNAMICS
Vol. 32, No. 3, May–June 2009

High-Capacity Tube Network Design Using the Hough Transform

Min Xue*
University of California, Santa Cruz, Moffett Field, California 94035
and
Parimal Kopardekar†
NASA Ames Research Center, Moffett Field, California 94035

DOI: 10.2514/1.40386

A new airspace design concept, tube networks, could enable high-density operations with less air traffic control workload. To construct tubes optimally, it is necessary to identify the commonality of flight trajectories. This paper proposes a new strategy to cluster great circle flight trajectories for forming tubes. The Hough transform is applied to identify groups or clusters of great circle trajectories that could form the tube networks. The genetic algorithm is then applied to optimize the tube network. Results show that small deviations from great circle routes could yield tubes that accommodate significant traffic levels within feasible computational time.

Nomenclature

d_{extra}	=	extra flight distance, %
d_1, d_2	=	distance, miles
R	=	radius of the Earth, miles
δ	=	latitude, deg
θ	=	angle, deg
λ	=	longitude, deg
ρ	=	distance, miles

I. Introduction

THE predicted growth in traffic demand over the next 20 years could result in increased congestion and delays in the National Airspace System (NAS). Under the dynamic airspace configuration (DAC) research sponsored by NASA [1], two major concepts, dynamic resectorization and corridors in the sky, or tube networks, have been proposed to ease congestion and delay. In the proposal, tubes will serve dense traffic that has similar trajectories. Assuming aircraft in tubes are capable of self-merging and self-separation, which would be true in future system, little air traffic control (ATC) workload is expected in tube operations. Thereafter, NAS capacity could be increased, and delay may be reduced. Developing tube networks is a promising concept due to its function of enabling high-density operations with less ATC workload [2]. Other potential benefits may include lower traffic flow management (TFM) restrictions, better predictability of flight operations, and fuel savings due to shorter routes.

Impenetrable tubes may result in additional costs for flights that need to be rerouted to avoid conflict with the traffic within the tubes. Thus, the number of tubes should not be too large. On the other hand, to be beneficial and efficient, the limited number of tubes should be able to accommodate large traffic levels and should not require tube users to fly too much extra distance to use the tube. To meet these three requirements: low numbers of tubes, large number of flights in the tubes, and low extra flight distances, it is important to observe and to identify the commonalities of the nationwide flight trajectories. If the number of flights that take common routes is large, constructing tubes based on these common routes will be valuable. Otherwise, tubes might not provide much advantage due to the confliction with the remaining traffic.

Several research efforts have focused on tube networks. Alipio et al. [2] and Yousefi et al. [3] suggested tubes based on city pairs by investigating the potential placement of tubes between two major cities such as Chicago and New York. If tubes are constructed based on city pairs, only a small portion of traffic will benefit with a limited number of tubes. Table 1 shows the flights among the top 25 U.S. airports vs the flights over the whole NAS on 20 April 2007. This network requires more than 200 links/tubes and can only serve at most 20% of the flights. Sridhar et al. [4] proposed a tube network interconnecting airports in clusters seeded by major airports to impact a significant amount of traffic. Although approximately 90% of flights are included, fully using the tubes may require too much extra flight distance for tube users, which could make this method prohibitive.

A new methodology that proposes a limited number of tubes base on observed patterns of flight trajectories is desired. In this work, consider trajectories that follow the great circle flight routes between city pairs. Several image/signal processing techniques for grouping flight patterns were investigated. Robelin et al. [5] developed an aggregation technique based on generalized principal component analysis (GPCA) [6] for constructing a model of air traffic flow directly from aircraft situation display to industry (ASDI) data. Martinez et al. [7] also used this aggregation technique to build a network flow graph. In these works, the authors used GPCA to get dominant directions at designated fixes from historical trajectories composed of series of waypoints/fixes. In this work, only origin and destination are considered for the great circle flight trajectory. Therefore, dimension reduction techniques like GPCA may not help. In computer vision and pattern recognition, the Hough transform [8–10] has been widely used for detecting lines, curves, or even geometric shapes that can be defined by parametric equations. Based on the point-line duality, the Hough transform can be used to transform great circle trajectories to points in another space. Points that are close to each other will likely correspond to great circle trajectories that are close enough to form a tube. Thus, the Hough transform is a good candidate for clustering great circle flight trajectories.

This paper presents a new methodology based on the Hough transform and genetic algorithm (GA) to observe and cluster

Presented as Paper 7396 at the AIAA Guidance, Navigation, and Control Conference, Honolulu, HI, 18–21 August 2008; received 12 August 2008; revision received 29 December 2008; accepted for publication 5 January 2009.

*Research Scientist, Mail Stop 210-10; Min.Xue@nasa.gov. Member AIAA.

†Research Scientist, Automation Concepts Branch, Mail Stop 210-10; Parimal.H.Kopardekar@nasa.gov. Senior Member AIAA.

Table 1 Flights among top 25 U.S. airports

Altitude, ft	Flights among top 25 airports	Flights over U.S.	Percentage
>0	7,117	60,362	11.8%
>12,000	6,870	47,313	14.5%
>18,000	6,677	41,229	16.2%
>24,000	6,313	35,590	17.7%
>29,000	5,914	29,887	19.8%
>35,000	3,688	17,916	20.6%

common great circle flight routes. This work provides the basis for future construction by proposing the potential tubes. The results show that a limited number of tubes in the national airspace can accommodate significant flights with low extra flight distances for tube users. Furthermore, dynamic tube recognition can be fulfilled by executing such a procedure periodically.

II. Modeling and Architecture of Designing Tubes

In this section, the data used were discussed. The procedures for identifying and proposing the potential tubes that eventually compose the networks are briefly introduced as well.

A. Data Acquisition

Traffic data for this work were obtained from the FAA's ASDI for the entire day of 20 April 2007. The ASDI file for this day contains 62,143 flights. Because only the continental U.S. is of interest, a rectangular bounding box surrounding the continental U.S. is formed: the latitude range is [17.2°N, 50.0°N] and the longitude range is [225.8°E, 296.7°E]. For each flight, only the origin and destination are used for defining great circle flight routes. Without loss of generality, only flights with tracks above FL290 (FL stands for flight level) are taken into account. During preprocessing, the great circle flight trajectories are determined, and those trajectories that do not overfly the continental U.S. region are removed. These preprocessing steps result in a final total of 29,629 flights to be considered.

B. Procedure

The procedure to identify and generate tubes is shown in Fig. 1. First, the preprocessed great circle trajectories are transformed into points in Hough space. Each point corresponds to one great circle flight route. Next, initial clustering is performed by the voting scheme on the basis of those points, which is essentially a grid-based clustering. Because the criterion for clustering the trajectories is minimal excess flight distance instead of the Euclidian distance, the flights are removed from their clusters if there is too much extra flight distance. Based on these initial clusters, the GA is applied to refine the results by moving the centers of tubes to seek better clustering.

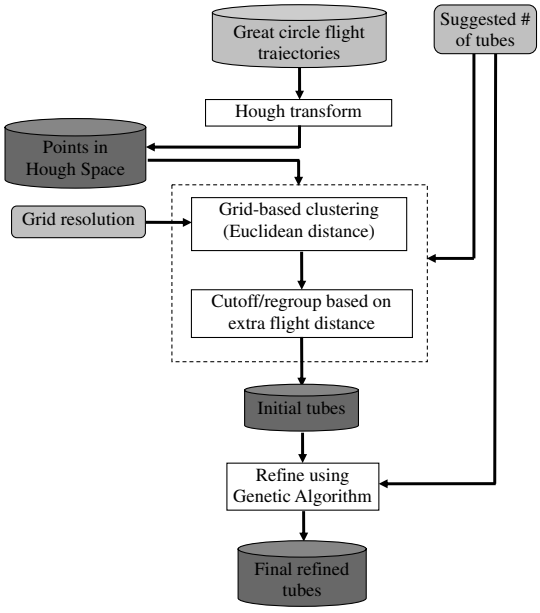

Fig. 1 Procedure to identify and generate tubes.

III. Methodology and Results

In this section the Hough transform and its parameterization are described first. After that, the initial clustering based on the voting scheme for the points in the Hough space is presented. On the basis of the initial clusters, the GA is applied to improve the design.

A. Hough Transform for Great Circle Routes

Polar representation of a line is referred to as Hough transform in image processing literature [9]. The equation to a line with the shortest distance ρ to the origin and an angle θ between its normal and the x axis is given by

$$\rho = x\cos\theta + y\sin\theta \tag{1}$$

The (x, y) are in Cartesian coordinates, and the (ρ, θ) are in the Hough space. This property is also called point-line duality.

Although a great circle line lies in three-dimensional space, it actually has only 2 degrees of freedom. Thus, it is suitable to apply the Hough transform. Given a flight with the origin at (δ_o, λ_o) and the destination at (δ_d, λ_d), assuming the Earth is an ideal sphere, the Cartesian coordinates will be

$$\mathbf{r}_i = \begin{bmatrix} x_i \\ y_i \\ z_i \end{bmatrix} = R \cdot \begin{bmatrix} \cos\lambda_i \cdot \cos\delta_i \\ \sin\lambda_i \cdot \cos\delta_i \\ \sin\delta_i \end{bmatrix} \tag{2}$$

where $i = o, d$ representing the origin and destination, respectively. R is the radius of the Earth, δ and λ are latitude and longitude, respectively, and x, y, and z are the Cartesian coordinates. Any point $\mathbf{r} = [x, y, z]^T$ on this great circle line should satisfy

$$\begin{cases} \mathbf{r}_o \times \mathbf{r}_d & = \mathbf{r} \times \mathbf{r}_d \\ \|\mathbf{r}\| & = R \end{cases} \tag{3}$$

Just as with straight lines, to transform the great circle lines a reference point has to be defined along with a reference axis. The reference point can be put anywhere inside of the bounding box, and the reference axis can point to any direction. Though different references generate different Hough transform results, they do not affect the nature of clustering as long as the references are fixed during the whole process. In this work, the reference point is set at [33.6°N, 261.3°E] (the center of the defined rectangular region), and the reference axis is defined to point the East. Figure 2 shows how ρ is defined as the shortest distance between the reference point and the great circle route and how θ is defined as the cross angle between the reference axis and the tangent vector at the reference point, which is aligned with ρ. Here $\rho \in [0, \infty]$ and $\theta \in [0, 2\pi]$. Detailed derivation of Hough and DeHough transforms for great circle routes are presented in the Appendix A.

Figure 3 shows the results after the Hough transform. The 29,629 great circle flight routes are transformed to points in Hough space. Some of them overlap each other. Apparently, the relationship among the trajectories can be easily told by the points in the Hough space. Notice how the points form many parabolalike curves in the

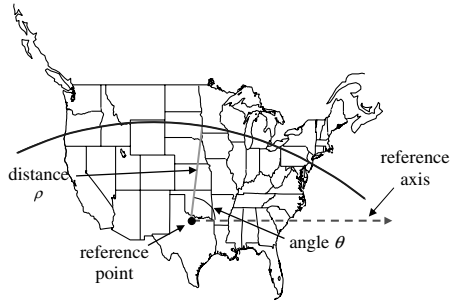

Fig. 2 Hough transform for great circle routes.

Hough space. This phenomenon can be explained using the point-line duality. Each curve essentially implies an airport, and the points forming the curve correspond to all the trajectories going through that airport. This supposition can be borne out by the following equation:

$$\rho = R \cdot \arctan\left[\tan\left(\frac{d}{R}\right) \cdot \cos(\gamma - \theta)\right] \tag{4}$$

where d is the shortest distance/great circle distance between an airport and the reference point. The variable γ is the angle between the line, which links the airport and the reference point, and the reference axis. The derivation can be found in the AppendixA. Given an airport, the values of d and γ, are fixed. Because the radius of Earth R is a constant, parameters ρ and θ have a fixed relationship. For instance, ORD (Chicago O'Hare International Airport) has $d = 826$ miles and $\gamma = 47.7$ deg, whereas JFK (New York JFK International Airport) has $d = 1451.8$ miles and $\gamma = 26.8$ deg. As shown in Fig. 3, all the trajectories going through these two airports fall on the blue and green curves, respectively.

B. Initial Results

In image processing, the continuous (ρ, θ) Hough space is then quantized into suitable size $(\Delta\rho \times \Delta\theta)$ grids and each grid is associated with an element of an array called the accumulator array. After this, the lines are extracted by the voting scheme. In this work, similar grids are constructed in the Hough space to catch the potential high-density tubes. Without loss of generality, the number of tubes is set to 60 in this work. The resolutions are defined as $\Delta\rho = 50$ miles and $\Delta\theta = 10$ deg. The 60 grids with the highest point density are shown as red rectangles in Fig. 4. They accommodate 59% of the 29,629 flights. After the Dehough transform, these 60 grids become 60 tubes. A sample tube from one of these grids is presented in Fig. 5a. The red curve/tube is transformed from a midpoint that is the average over all points inside of the grid in the Hough space. The blue curves are the actual great circle flight routes that can use this tube.

If the Hough coordinates of a flight trajectory are not exactly the same as the weighted center of its corresponding grid, there will be extra flight distance for the flight to use the designated tube. On the other hand, due to the finite length, the great circle routes have largely varied extra distances even if the coordinates in $(\rho - \theta)$ space are the same. Therefore, the extra distance, which is assumed to be the main concern of the tube users, should serve as the criteria for clustering instead of the Euclidean distance. The extra distance must be calculated in the original space, because the origin and destination are lost in the transformation. The extra flight distance, shown in Fig. 5b, is defined as a rate

$$d_{\text{extra}} = \frac{d_1 + d_2}{D} \cdot 100\% \tag{5}$$

where d_i are the shortest distances to join or leave the tube, and D is the original great circle flight distance. Figure 5b demonstrates that if the flight with the blue trajectory uses the red tube, it will have d_{extra} percent of deviation from its shortest distance.

Most of the clustering algorithms suitable for Euclidean distance will not be efficient for the extra flight distance due to the complexity of the relative positions with the extra flight distance. Even a stochastic-process-based optimization algorithm, like the GA, cannot determine the optimal solutions in a feasible computational time without a good initial guess. The search will be exhaustive and the required computational time will make it prohibitive. Fortunately, clustering based on Euclidean distance in the Hough space should be a rough estimate of the clustering based on the extra distance in the original space. For instance, if two trajectories are far away from each other in the Hough space, they most likely have large extra distance. On the other hand, if they are far from each other in the $\rho - \theta$ space, the probability of having low extra distance between them is low.

Thus, the clustering results based on Euclidean distance in the Hough space is used, and the flights that have higher extra distance in original space than a defined threshold are removed. If the tolerable extra flight distance is defined as 5% of the shortest flight distance, the percentage of flights that top 60 tubes can hold drops from 59% to 31%. The large decrease indicates the difference between two clustering criteria. Figure 6 displays the top 60 tubes. In this figure, only the portions that have more than 60 flights are shown.

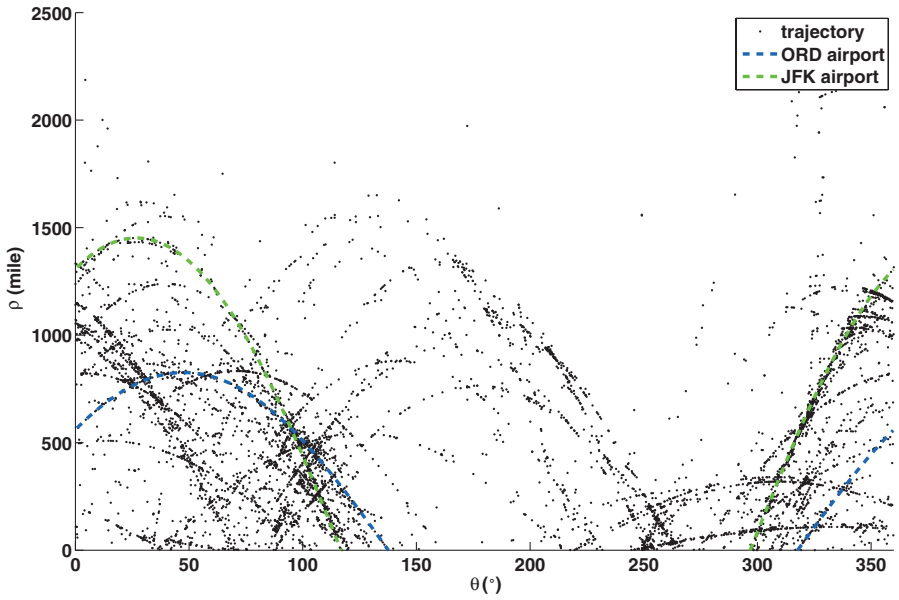

Fig. 3 Transformed trajectories as points in Hough space.

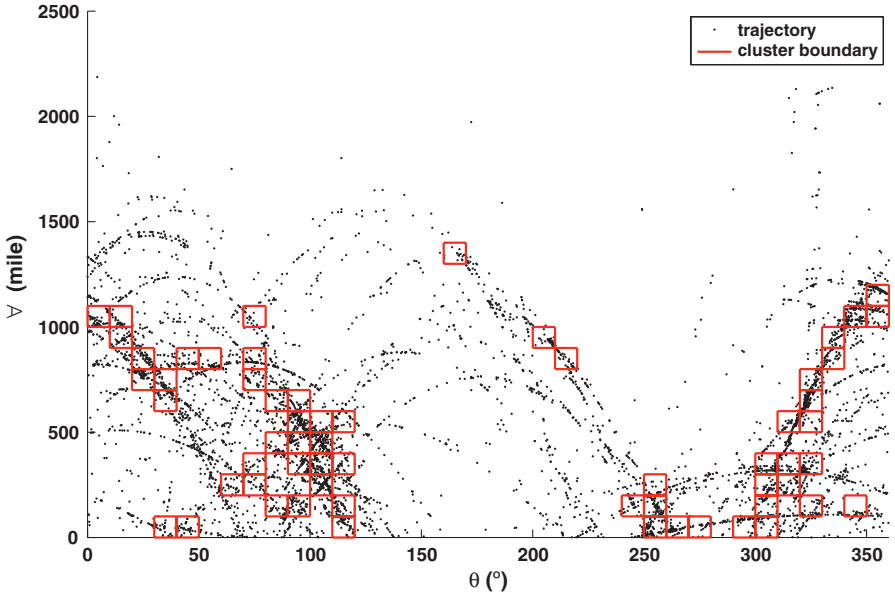

Fig. 4 ORD and JFK in Hough space and the initial top 60 grids based on Hough transform.

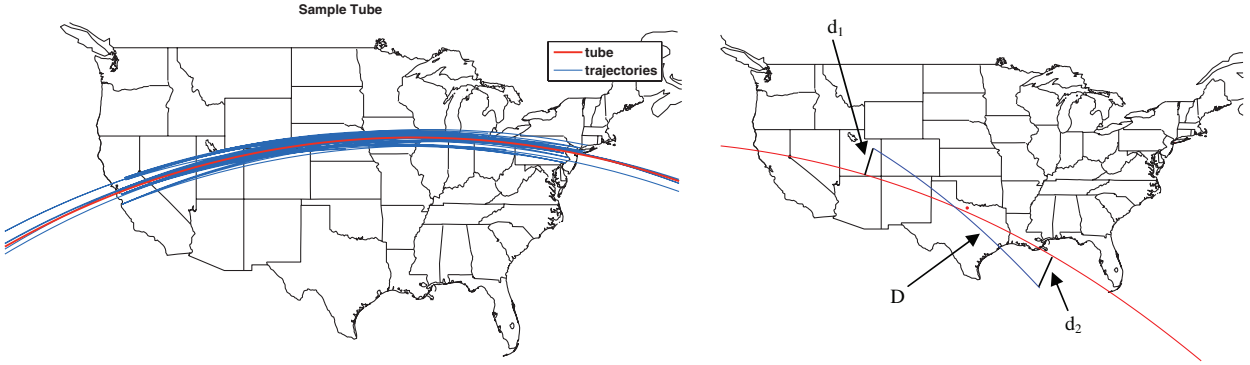

a) A sample of the tube

b) Definition of extra flight distance

Fig. 5 Tube and extra distance.

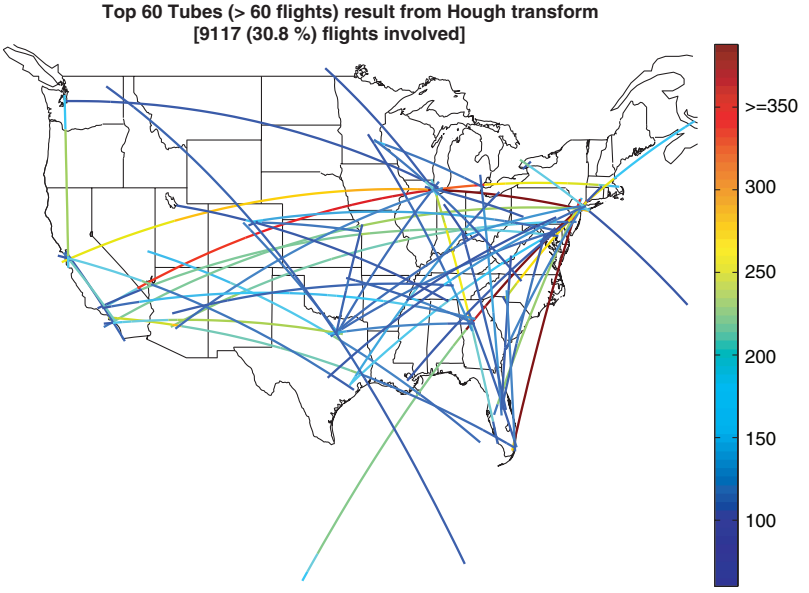

Fig. 6 Top 60 tubes based on Hough transform.

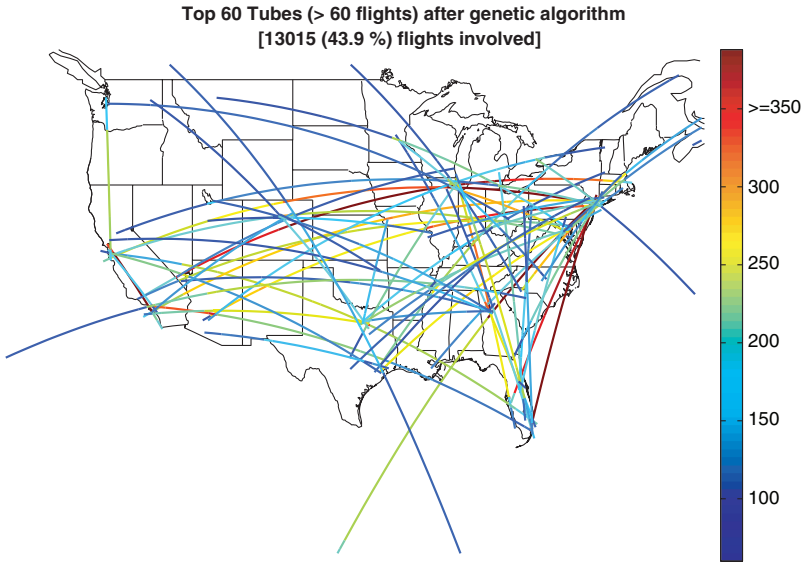

Fig. 7 Top 60 tubes after refining using GA.

A warmer color denotes higher density of the traffic, whereas a colder color represents lower density. The density of the traffic can be judged by the color bar.

C. Refinement Using Genetic Algorithm

To maximize the number of benefited flights, an optimization algorithm is applied to these initial tubes. In this work, the GA is used to optimize the clustering, because it has been widely used as a powerful optimization method.

The GA is a stochastic process that models two natural phenomena: genetic inheritance and Darwinian evolution [11]. It first creates a population of potential solutions. Each solution is called a "chromosome," represented by a binary string of length $m = \sum_{i=1}^{k} m_i$, where k is the number of design parameters. The first m_i bits of the string correspond to the first design parameter, or "gene." The next group with m_i bits will map to the second design parameter, and so on. In each generation, the population of chromosomes will be evaluated by using a cost function. The new population is selected with respect to the probability distribution based on fitness values. Finally, the chromosomes are altered in the new population by mutation and crossover operators.

In this work, the weighted centers of the grids in the Hough space are optimized. Because each center has two coordinates ρ and θ, the number of optimization parameters will be 120. The clustering results from the Hough transform discussed previously will serve as initial values for the GA. For the selection process inside of the GA, a roulette wheel with slots sized according to fitness is used. The crossover probability is 0.8 and mutation probability is 0.2. The population size is set to 200, and it will stop after 200 generations. The threshold for the extra flight distance is 5%.

After 200 generations, the percentage of flights that the top 60 tubes can accommodate increases from 31 to 44%. The grid centers did not change dramatically, which means the original clustering provided a good start. Figure 7 shows the final top 60 tubes. Only the portions that have more than 60 flights are displayed. On the platform of MacOS with Intel Core 2 Duo Processor 3.0 GHz, 200 generations takes around 10 h with 4 threads working in parallel. This computation time can be shorten by lowering the number of generations or running the GA in more powerful parallel computing clusters.

D. Analysis

To get insight into the operations in the tubes, the flights within the designed tubes are investigated. Figure 8 shows the flights between any two of the top 25 airports vs the rest in each tube. Similar to the observation in Sridhar et al. [4], it is noticed that flights among these airports do not account for a major portion of the total operations within the tubes. These results further testify to the importance of building tubes upon the nature of flight trajectories vs major-city pairs.

This study focused on flights over FL290. Several other partitions are explored in an altitude sensitivity analysis. Based on a 5% deviation, Table 2 presents the results for all flights that are flying above a given altitude. The results show that flights at high altitudes have stronger tube conformance than those at low altitudes, which

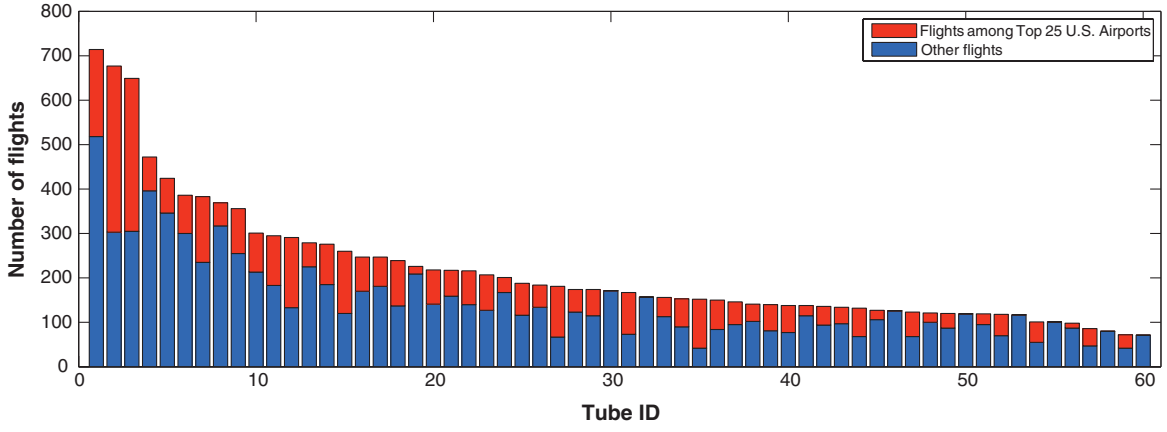

Fig. 8 Percentage of flights among top 25 U.S. airports.

Table 2 Flights included in tubes given 5% deviation

Altitude, ft	Flights involved	Percentage
>0	17,274	29%
>24,000	14,485	41%
>29,000	13,015	44%
>35,000	8,658	49%

implies that it may be more valuable to construct tubes/corridors at high altitudes than at low altitudes.

The sensitivity analysis can be conducted if the deviation constraints are varied. Table 3 presents the relationship between the deviation constraints and the number of flights included in the tubes based on flights over FL290. The results demonstrate that the more deviation allowed from the shortest distance, the more flights can be included into the tubes. This provides us a profile of the benefits pool of constructing tube networks. Although the largest deviation can yield about 70% flights operated in the tubes, it should be carefully decided in practice and weighed against the cost of deviating.

IV. Conclusions

Identifying tubes that catch the commonalities of the shortest distance trajectories is necessary for constructing tubes/corridor-in-the-sky structures in future airspace. If the clustering is based on the city pairs to cluster, only a small amount of traffic per tube might benefit. Building tube network clusters by seeding them with major cities increases the benefit pool but requires too much extra flight distance for the tube users. Clustering the trajectories directly can identify the potential tubes that provide a compromise between the benefit pool and the extra flight distance required.

In this work, a new methodology is developed based on the Hough transform, which enables the clustering of great circle flight routes. Extra flight distance beyond the shortest flight distance serves as the criteria for clustering. The Hough transform generates good initial guesses, and thereafter, GA refines the tubes if the restriction of computational time allows. Results show that significant traffic would benefit from the tubes by only using a small number of tubes. Using these tubes only requires 5% extra flight distances. The entire process could be achieved within a feasible computational time. This procedure could be directly used for dynamic tube design if the data are fed in during incremental time periods. The list of tubes proposed by our method can be used as a basis. With further constructional and operational analysis, the final tubes or network can be eventually constructed. This method can be applied to the wind optimal trajectory if the wind velocity is constant for the entire trajectory. In future work, efforts will be put on general wind optimal trajectories.

Appendix: Hough-Transform Related Calculations

As described in Fig. A1, given a great circle flight route composed of two points/airports $(\mathbf{u}, \mathbf{v})$, to get the unique Hough transform, a reference point $\mathbf{p}$ is first configured, which has geographic coordinates, latitude (δ_p) and longitude (λ_p), and Cartesian

Table 3 Flights included in tubes given varied deviation

Deviation	Flights involved	Percentage
1%	3,692	13%
2%	6,736	23%
3%	8,998	30%
4%	11,265	38%
5%	13,015	44%
7%	16,085	54%
9%	18,666	63%
11%	20,407	69%

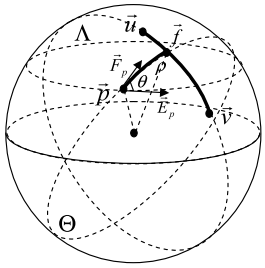

Fig. A1 Calculation of the Hough transform.

coordinates $[p_1, p_2, p_3]^T$. In this work, the ρ, one parameter in the Hough transform, is defined as the shortest distance between point $\mathbf{p}$ and the given great circle on the sphere/Earth surface. Assume the great circle plane Λ containing $\mathbf{u}$ and $\mathbf{v}$ has norm $\mathbf{n}_\Lambda\ [n_{\Lambda 1}, n_{\Lambda 2}, n_{\Lambda 3}]^T$. If we create another great circle plane Θ, which includes reference point $\mathbf{p}$ and is perpendicular to existing plane Λ, then ρ will be the great circle distance between $\mathbf{p}$ and the closer intersection point $\mathbf{f}$ ($[\delta_f, \lambda_f]$ and $[f_1, f_2, f_3]^T$). Furthermore, we define the tangent vector $\mathbf{E}_p$ at point $\mathbf{p}$, which points East, to be the base direction. Thus, another parameter in Fough transform θ is defined as the cross angle between vector $\mathbf{E}_p$ and the tangent vector $\mathbf{F}_p$ at point $\mathbf{p}$, which lies in the great circle plane Θ.

I. Calculation of ρ in Hough Transform

To compute ρ, we first need to find the intersection points mentioned previously. Then, the closer one is chosen. Assume the points are $\mathbf{f}_A(\delta_{f_A}, \lambda_{f_A})$ and $\mathbf{f}_B(\delta_{f_B}, \lambda_{f_B})$. δ and λ should satisfy the following equations:

$$\cos\lambda \cdot n_{\Lambda 1} + \sin\lambda \cdot n_{\Lambda 2} + \tan\delta \cdot n_{\Lambda 3} = 0 \tag{A1a}$$

$$\begin{bmatrix} p_2 \cdot \tan\delta - p_3 \cdot \sin\lambda \\ p_3 \cdot \cos\lambda - p_1 \cdot \tan\delta \\ p_1 \cdot \sin\lambda - p_2 \cdot \cos\lambda \end{bmatrix} \cdot \begin{bmatrix} n_{\Lambda 1} \\ n_{\Lambda 2} \\ n_{\Lambda 3} \end{bmatrix} = 0 \tag{A1b}$$

If $p_2 \cdot n_{\Lambda 1} - p_1 \cdot n_{\Lambda 2} \neq 0$, from Eq. (A1b), it can be derived

$$\tan\delta = \frac{-\sin\lambda(p_1 n_{\Lambda 3} - p_3 n_{\Lambda 1}) - \cos\lambda(p_3 n_{\Lambda 2} - p_2 n\Lambda 3)}{(p_2 n_{\Lambda 1} - p_1 n_{\Lambda 2})} \tag{A2}$$

by substituting Eq. (A2) in Eq. (A1a) we have

$$[(p_2 n_{\Lambda 1} - p_1 n_{\Lambda 2}) n_{\Lambda 1} - (p_3 n_{\Lambda 2} - p_2 n_{\Lambda 3}) n_{\Lambda 3}]\cos\lambda + [(p_2 n_{\Lambda 1} - p_1 n_{\Lambda 2}) n_{\Lambda 2} - (p_1 n_{\Lambda 3} - p_3 n_{\Lambda 1}) n_{\Lambda 3}]\sin\lambda = 0 \tag{A3}$$

by defining

$$A = (p_2 n_{\Lambda 1} - p_1 n_{\Lambda 2}) n_{\Lambda 2} - (p_1 n_{\Lambda 3} - p_3 n_{\Lambda 1}) n_{\Lambda 3} \tag{A4a}$$

$$B = (p_2 n_{\Lambda 1} - p_1 n_{\Lambda 2}) n_{\Lambda 1} - (p_3 n_{\Lambda 2} - p_2 n_{\Lambda 3}) n_{\Lambda 3} \tag{A4b}$$

Given the reference point $\mathbf{p}$ and U.S. region interested, we have

$$A^2 + B^2 > 0 \tag{A5}$$

Equation (A3) then becomes

$$\sin(\lambda + \beta) = 0 \tag{A6}$$

where

$$\cos\beta = \frac{A}{\sqrt{A^2 + B^2}} \tag{A7a}$$

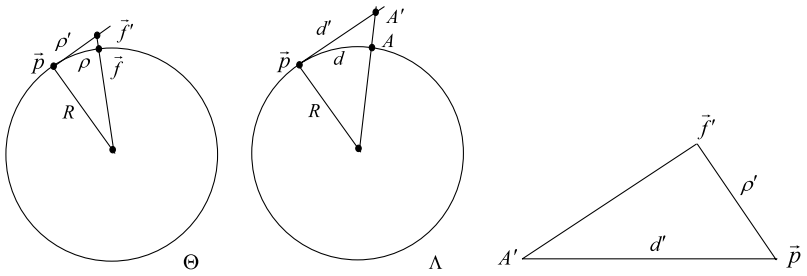

a) Plane Θ **b) Plane Λ** **c) Triangle**

Fig. A2 Calculation of the relationship for trajectories via an airport.

$$\sin\beta = \frac{B}{\sqrt{A^2 + B^2}} \tag{A7b}$$

Eventually, we get $\lambda = k\pi - \beta,\ k = [\cdots\ -1\ \ 0\ \ 1\ \cdots]$, where $\lambda \in [0, 2\pi]$. Because there only exists two values between 0 and 2π, define them to be λ_1 and λ_2, respectively.

$$\delta_i = \arctan\left[-\frac{\cos\lambda_i n_{\Lambda 1} + \sin\lambda_i n_{\Lambda 2}}{n_{\Lambda 3}}\right] \tag{A13}$$

where $i = 1, 2, 3, 4$.

If $n_{\Lambda 3} = 0$, then the great circle route should have constant longitude, which means the latitudes of intersection points should be equal to δ_p.

Finally, the latitude and longitude of the intersection point for shortest distance ρ can be concluded

$$(\delta_f, \lambda_f) = \begin{cases} \arg\min_{\substack{\delta\in[\delta_1,\delta_2]\\ \lambda\in[\lambda_1,\lambda_2]}}[\text{great}_{\text{circle}}\text{dist}((\delta,\lambda),\mathbf{p})] & \text{if } p_2\cdot n_{\Lambda 1} - p_1\cdot n_{\Lambda 2} \neq 0 \quad \text{and} \quad n_{\Lambda 3} \neq 0, \\ \arg\min_{\lambda\in[\lambda_1,\lambda_2]}[\text{great}_{\text{circle}}\text{dist}((\delta_p,\lambda),\mathbf{p})] & \text{if } p_2\cdot n_{\Lambda 1} - p_1\cdot n_{\Lambda 2} \neq 0 \quad \text{and} \quad n_{\Lambda 3} = 0, \\ \arg\min_{\substack{\delta\in[\delta_3,\delta_4]\\ \lambda\in[\lambda_3,\lambda_4]}}[\text{great}_{\text{circle}}\text{dist}((\delta,\lambda),\mathbf{p})] & \text{if } p_2\cdot n_{\Lambda 1} - p_1\cdot n_{\Lambda 2} = 0 \quad \text{and} \quad n_{\Lambda 3} \neq 0, \\ \arg\min_{\lambda\in[\lambda_3,\lambda_4]}[\text{great}_{\text{circle}}\text{dist}((\delta_p,\lambda),\mathbf{p})] & \text{if } p_2\cdot n_{\Lambda 1} - p_1\cdot n_{\Lambda 2} = 0 \quad \text{and} \quad n_{\Lambda 3} = 0, \end{cases} \tag{A14}$$

If $p_2 \cdot n_{\Lambda 1} - p_1 \cdot n_{\Lambda 2} = 0$, from Eq. (A1b), we get

$$-\sin\lambda(p_1 n_{\Lambda 3} - p_3 n_{\Lambda 1}) - \cos\lambda(p_3 n_{\Lambda 2} - p_2 n_{\Lambda 3}) = 0 \tag{A8}$$

by defining

$$C = -(p_1 n_{\Lambda 3} - p_3 n_{\Lambda 1}) \tag{A9a}$$

$$D = -(p_3 n_{\Lambda 2} - p_2 n_{\Lambda 3}) \tag{A9b}$$

Again, given the reference point $\mathbf{p}$ and the U.S. region of interest, we have

$$C^2 + D^2 > 0 \tag{A10}$$

Then, rewrite Eq (A8) in simpler form

$$\sin(\lambda + \gamma) = 0 \tag{A11}$$

where

$$\cos\gamma = \frac{C}{\sqrt{C^2 + D^2}} \tag{A12a}$$

$$\sin\gamma = \frac{D}{\sqrt{C^2 + D^2}} \tag{A12b}$$

Similarly, we have $\lambda = k\pi - \gamma,\ k = [\cdots\ -1\ \ 0\ \ 1\ \cdots]$, where $\lambda \in [0, 2\pi]$. Again, define the two values between 0 and 2π to be λ_3 and λ_4, respectively.

Now, δ can be computed explicitly. If $n_{\Lambda 3} \neq 0$, from (A1a), we can derive

Where the operator "great_circle_dist" computes the great circle distance between the pair of geographic coordinates.

II. Calculation of θ in Hough Transform

Next, the cross angle θ between vector $\mathbf{E}_p$ and $\mathbf{F}_p$ is computed. Assuming the normal of the great circle plane Θ is $\mathbf{n}_\Theta$, where

$$\mathbf{n}_\Theta = \mathbf{n}_\Lambda \times \mathbf{p} \tag{A15}$$

the vector $\mathbf{F}_p$ can be computed by

$$\mathbf{F}_p = \mathbf{n}_\Theta \times \mathbf{p} \tag{A16}$$

Assuming the great circle plane that $\mathbf{E}_p$ lies in is plane Γ and its normal is $\mathbf{n}_\Gamma$ (actually normalized form is $[0, 0, 1]^T$), by defining the projection of $\mathbf{p}$ in the horizontal plane, which contains the equator, as $\mathbf{p}[p_1, p_2, 0]^T$, we get

$$\mathbf{E}_p = \mathbf{n}_\Gamma \times \mathbf{p}' \tag{A17}$$

Then, the θ' within $[0, \frac{\pi}{2}]$ is computed:

$$\theta' = \arccos\left(\frac{\mathbf{E}_p \cdot \mathbf{F}_p}{|\mathbf{E}_p| \cdot |\mathbf{F}_p|}\right) \tag{A18}$$

By checking the relative position between point $\mathbf{p}$ and $\mathbf{f}$, we can finally get θ explicitly.

III. Dehough Transform

Given a Hough transform point with θ and ρ, by simply reversing the procedures of the preceding Hough transform with the same reference point, reference direction, and interested region, we can

compute the great circle flight route with two end points on the boundary of the defined region.

IV. Relationship Among the Trajectories Going Through an Airport

Defining a reference point $\mathbf{p}(\delta_p, \lambda_p)$ and axis pointing to the East, and specifying an airport $\mathbf{A}(\delta_A, \lambda_A)$ (see Fig. A2, we could find the relationship between ρ and θ for any great circle routes going through the airport.

For any great circle route via airport $\mathbf{A}$, suppose f is the perpendicular foot on the great circle line, which makes $\widehat{pf} \perp \widehat{Af}$. Define the plane that is tangent to the earth at point $\mathbf{p}$ as plane Π. Assuming the origin of Earth is O, on plane Π, define that A' and f' are the points collinear with $\overline{OA}$ and $\overline{Of}$, respectively. For the right triangle $\Delta A' f' P$, we have

$$\rho' = \overline{pf'} = R \cdot \tan\gamma = R \cdot \tan\left(\frac{\rho}{R}\right) \tag{A19}$$

and

$$d' = \overline{pA'} = R \cdot \tan\left(\frac{d}{R}\right) \tag{A20}$$

Assuming the great circle distance/shortest distance between $\mathbf{p}$ and $\mathbf{A}$ is d, and the angle between the norm of route and the reference axis is γ, the relationship between ρ and θ can be expressed as

$$\rho' = d' \cdot \cos(\gamma - \theta)] \tag{A21}$$

then we can get Eq. (4).

References

[1] Kopardekar, P., Bilimoria, K., and Sridhar, B., "Initial Concepts for Dynamic Airspace Configuration," *7th AIAA Aviation Technology, Integration and Operations Conference (ATIO)*, AIAA Paper 2007-7763, Sept. 2007.

[2] Alipio, J., Castro, P., Kaing, H., Shahd, N., Sheizai, O., Donohue, G. L., and Grundmann, K., "Dynamic Airspace Super Sectors (DASS) as High-Density Highways in the Sky for a New US Air Traffic Management System," *AIAA/IEEE Digital Avionics Systems Conference*, AIAA, Reston, VA, Oct. 2003, pp. 57–66.

[3] Yousefi, A., Donohue, G. L., and Sherry, L., "High-Volume Tube-Shape Sectors (HTS): A Network of High Capacity Ribbons Connecting Congested City Pairs," *Proceedings of the 23rd Digital Avionics Systems Conference*, IEEE Publications, Piscataway, NJ, 2004, pp. 3:1–7.

[4] Sridhar, B., Grabbe, S., Sheth, K., and Bilimoria, K. D., "Initial Study of Tube Networks for Flexible Airspace Utilization," *AIAA Guidance, Navigation, and Control Conference and Exhibit*, AIAA Paper 2006-6768, Aug. 2006.

[5] Robelin, C., Sun, D., Wu, G., and Bayen, A. M., "MILP Control of Aggregate Eulerian Network Airspace Models," *Proceedings of the American Control Conference*, Minneapolis, MN, June 2006.

[6] Vidal, R., Ma, Y., and Sastry, S., "Generalized Principal Component Analysis (GPCA)," *IEEE Conference on Computer Vision and Pattern Recognition*, IEEE Publications, Piscataway, NJ, June 2003, pp. 621–628.

[7] Martinez, S. A., Chatterji, G. B., Sun, D., and Bayen, A. M., "A Weighted-Graph Approach for Dynamic Airspace Configuration," *AIAA Guidance, Navigation and Control Conference and Exhibit*, AIAA Paper 2007-6448Aug. 2007.

[8] Hough, P. V. C., Method and Means for Recognizing Complex Patterns, U.S. Patent No. 3069654, 1962.

[9] Duda, P. E., and Hart, R. O., "Use of the Hough Transformation to Detect Lines and Curves in Pictures," *Communications of the ACM*, Vol. 15, No. 1, 1972, pp. 11–15. doi:10.1145/361237.361242

[10] Trucco, E., and Verri, A., *Introductory Techniques for 3-D Computer Vision*, Prentice–Hall, Upper Saddle River, NJ, 1998, pp. 97–101.

[11] Michaelwicz, Z., *Genetic Algorithms + Data Structures = Evolution Programs*, 3rd ed., Springer–Verlag, Berlin, 1996, pp. 11–30, Chap. 1.